Available online at www.sciencedirect.com
ScienceDirect
ELSEVIER
Journal of the European Ceramic Society 27 (2007) 1919–1925
www.elsevier.com/locate/jeurceramsoc

Thermal shock of alumina by compressed air cooling

F. Hugot [a,*], J.C. Glandus [b]

[a] *Laboratoire de Rhéologie du Bois de Bordeaux, UMR 5103, INRA, CNRS, Université Bordeaux 1, Domaine de l'Hermitage, 69 Route d'Arcachon, 33612 Cestas, France*
[b] *ENSCI, 47 Avenue Albert Thomas, 87065 Limoges, France*

Received 15 March 2006; received in revised form 23 June 2006; accepted 30 June 2006
Available online 27 September 2006

Abstract

Alumina samples has been submitted to mild thermal shocks by quenching in a compressed air flow and the critical temperature difference has been determined for increasing thermal shock severities. Then these critical shocks have been numerically simulated by varying the superficial heat exchange coefficient value until the maximal tensile stress reaches the material strength. The combination of experimental and numerical approaches leads to indirect estimate of the heat exchange coefficient values during the tests.

Keywords: Al_2O_3; Thermal shock resistance; Failure analysis; Exchange coefficient

1. Introduction

Many theoretical and experimental works have been devoted to the study of the thermal shocks resistance of ceramics subjected to water quench. All of them allow to characterize the behaviour of these materials in conditions of exceptionally severe solicitation, but very far from those induced by actual conditions of use. They lead to the knowledge of the smallest temperature difference entailing the ruin of a sample under a single quench that is to say to an ultimate characteristic of the material.

In conditions of use, the failure of a ceramic component under a single excessively severe thermal shock is unacceptable. On the other hand, its ruin in thermal fatigue induced by the repetition of mild thermal shocks is unavoidable. So it is of interest to study the resistance of such materials in conditions of moderated heat exchanges in order to characterize their behaviour in real service conditions.

Two elementary theories are often used to account for global effects of a thermal shock:

- the thermoelastic theory[1] supposes that the material, originally uncracked, cracks when the thermal stress level exceeds, locally, its strength;
- the energetic theory[2] considers the material initially microcracked and studies the stability of these flaws in the thermal stress field.

Although coarse and little respectful of the microstructural ceramics specificities, these two approaches constitute efficient tools in the experimental result interpretation.

On the basis of a thermoelastic approach, the present paper characterizes the resistance of a structural ceramic submitted to mild thermal shocks (cooling by compressed air) and it compares the results thus obtained to the performances of the same material in more severe thermal shock conditions (water quench).

From a thermoelastic viewpoint, a solid quenched from the initial temperature T_i; to the final temperature T_f, endures thermal stresses, σ_{th} equal to

$$\sigma_{th} = \Psi E\alpha\,\Delta T_f(\nu) \quad (1)$$

with $\Delta T = T_i - T_f$ and cracking occurs when the imposed temperature difference reaches the critical value ΔT_c such that:

$$\Delta T_c = \Psi^{-1}\frac{\sigma_R}{(E\alpha f(\nu))} \quad (2)$$

with Ψ is the stress reduction coefficient ($0 <= \Psi <= 1$), σ_R the strength, E the Young's modulus, α the linear expansion coefficient, ν the Poisson's ratio, $f(\nu)$ is the function of the Poisson's ratio and the sample geometry.

* Corresponding author.
E-mail address: hugot@lrbb3.pierroton.inra.fr (F. Hugot).

0955-2219/$ – see front matter © 2006 Elsevier Ltd. All rights reserved.
doi:10.1016/j.jeurceramsoc.2006.06.012

In each cross section of an infinite bar, in a plane strains state:[3]

$$f(\nu) = 1 - \nu, \quad \text{and} \quad \Psi^{-1} = 1.45 + \frac{4}{\beta} - 0.45\,\exp\left(-\frac{16}{\beta}\right) \tag{3}$$

with β is the Biot's number, characteristic of the shock severity ($\beta = ah/\lambda$), a the typical dimension of the sample, h the superficial heat exchange coefficient and λ is the thermal conductivity.

The first thermal shock resistance parameter, R, is defined by

$$R = \frac{\sigma_R}{(E\alpha f(\nu))} \tag{4}$$

$$\Delta T_c = \Psi^{-1} R \tag{5}$$

The practical use of these results is commonly fussy, chiefly because the numerical value of the heat exchange coefficient h is never well known. One aim of this work is precisely to suggest a method to estimate this parameter.

For this, a double approach, experimental and numerical, has been developed. For various conditions of cooling, the ΔT_c values have been determined experimentally. The temperature range, in which fracture occurs, was determined when a unique longitudinal crack appears on the main face only. Then, each of these critical shocks has been numerically simulated by adjusting the h value until the maximal calculated tensile stress reaches the material strength.

2. Materials and samples

Samples of a polycristalline alumina of commercial quality (Degussa AL23) have been used for this study. The main thermomechanical and physical properties of this material are listed:

Purity[a]	99.7%
Density[a]	3.7
Poisson's ratio[a]	0.25
Linear expansion coefficient[a]	About $8.1 \times 10^{-6}\,K^{-1}$ between 0 and 1000 °C
Thermal conductivity[a]	Between 30 W/mK (20 °C) and 5 W/mK (1000 °C)
Elastic modulus[b]	360 GPa
Mean tensile strength[b]	160 MPa

[a] Bibliography value.
[b] Value measured or calculated value.

Starting from plates (50 mm × 50 mm × 4 mm), bars of square cross section (4 mm × 4 mm × 36 mm) were obtained by sawing. Then, before the tests, the lateral corners of these bars were carefully bevelled to delete occasional defects. Circular cross sectional samples (ϕ = 6 mm) were also made by cutting long cylinders of the same material.

3. Experimentation

The objective was to submit the samples to decreasing thermal shocks by quenching them using compressed air, and to determine the critical temperature difference (ΔT_c) for each experimental condition. Characterisation was conducted onto a set of 10 specimens for each assumption test.

The tests were performed by using an automated bench of thermal shocks, conceived and built in the laboratory.[4] This bench, fully driven by a micro computer, assumes three main functions:

- The heating of samples in an electrical furnace with Kanthal coil (T_{max} = 1200 °C) and provided with upper and lower obturators limiting the chimney effects. The upper temperature of the thermal shock equal to the temperature of the oven and the lower temperature is measured during the test with a temperature sensor located inside the oven.
- The quenching of samples by cooling in a flow of compressed air (p_{max} = 6 bars).
- The cooling device consists of three nozzles located at 120° one to the other and fixed on a lathe chuck. This setting allows to impose simultaneously the same displacement to the three cooling nozzles and to maintain each of them to the same distance from the axis of the tested sample. In the case of squared section samples, one of the three nozzles is oriented perpendicularly to a face of the sample: it is called the main nozzle whereas the others are called the secondary nozzles. Specimen are held in grip jaw while taking them out from the oven and vertically fixed during the test.
- The transfer of samples by means of pneumatic actuators.

The macroscopic cracking of samples submitted to critical thermal shocks was observed by visual inspection by means of a dye penetrant method (Ardrox range products).

Among the numerous experimental parameters which play an obvious role on the thermal shock severity, one must quote chiefly: the sample geometry, the nozzle to sample distance, the number and the geometry of nozzles as well as the pressure of compressed air. For the present work, the influence of all these parameters has been studied, except that of air pressure, always constant at six bars.

Tests have been carried out on samples of square and circular cross section, submitted to the cooling of three cylindrical nozzles of 2.45 mm^2 cross section, then to the cooling of three cylindrical nozzles of 4.9 mm^2 cross section and finally to that of six cylindrical nozzles (two times two superposed nozzles) of 2.45 mm^2 cross section.

For each of these experimental settings, the critical drop in temperature, ΔT_c, has been measured.

4. Numerical simulation

The previous analytic approaches described in the introduction characterize the final state according both to the initial state and the thermal shock conditions: therefore they give a global description of the thermal shock only. On the other hand, the numerical calculation gives the state of stresses and temperatures at each time and for any point in the sample.

The present work uses the capabilities of the numerical code ABAQUS whose performances are well established in the field of linear and non-linear thermomechanical analysis. The tem-

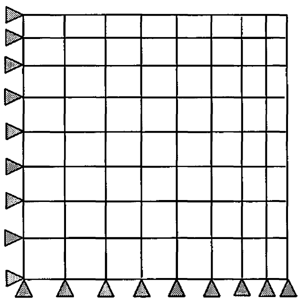

Fig. 1. Typical meshing of squared and circular cross sections.

perature dependence of thermal conductivity was considered in the simulation.

A quenched sample is supposed in a plane strain state: therefore it is sufficient to consider one of its cross sections. Moreover, because of the geometrical symmetries, it suffices to consider a quarter of this section, only, if the thermal loading respects the geometrical symmetry. Otherwise the whole section must be modelised.

As shown by the Fig. 1, a non-uniform meshing has been used in order to obtain a more accurate estimate of the superficial stresses level. On the same figure, one observes that, except in the vicinity of the axis of cylindrical samples, 8 nodes quadrilateral elements have been used, thus avoiding the need of a very fine meshing.

The Fig. 2 represents, for a squared and circular cross section samples, the relative position of a sample in the flow of compressed air. In the case of square section, it may be thought that the cooling of the main face (face in regard of the main nozzle) is better than those of secondary faces because this face is submitted to a normal impact of compressed air. This assumption is confirmed by experimental observations which show that the cracking develops always by priority along the main face. To take this behaviour into account, two numerical models of square sectional samples have been developed:

- in the first (model 1), the four faces of the sample are submitted to the same thermal loading;
- in the second (model 2), the three secondary faces are submitted to a thermal loading equal to 3/4 of that imposed on the main face.

For cylindrical samples a single modelisation has been developed: uniform thermal loading, perpendicular to the external surface.

5. Results and discussion

5.1. Critical temperature difference

The Fig. 3 represents, for all the cases studied, the variations of the measured ΔT_c according to the distance d (nozzles to sample distance) when this parameter varies from 2 to 25 mm. From a general standpoint, one notes that all the curves exhibit

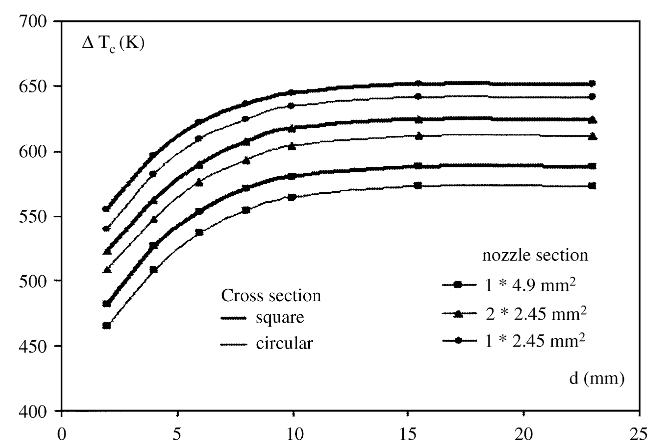

Fig. 3. Critical temperature difference vs. nozzle to sample distance for various experimental conditions.

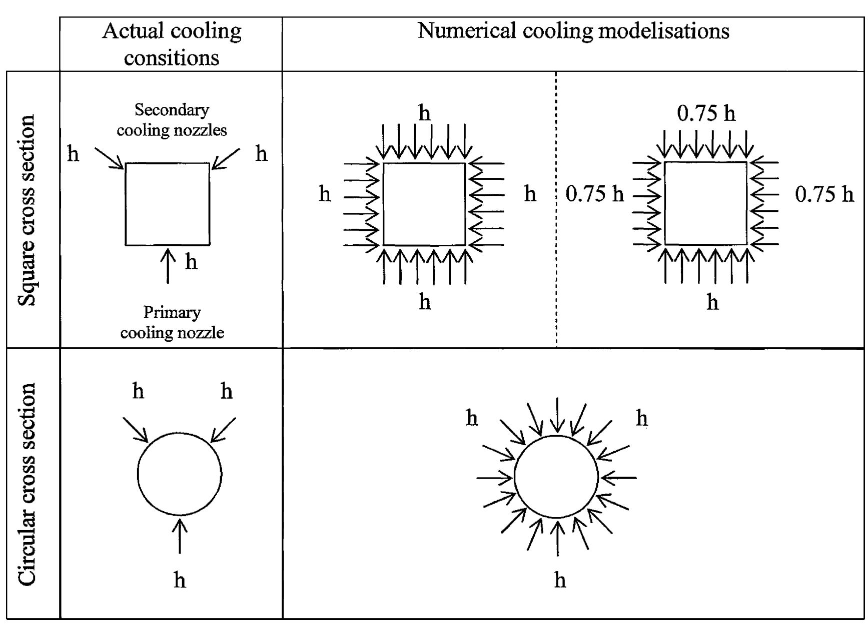

Fig. 2. Actual and modelled heat exchanges (h, superficial heat exchange coefficient).

the same trend ΔT_c increases rapidly for the weak d values then it tends to an asymptotic value which is quite reached for $d = 15$ mm.

One observes also that, for given experimental conditions, the curves dealing with cylindrical bars are slightly offsetted downward as compared to those dealing with square sectional bars. This gap, which indicates a greater severity of thermal shocks in the case of cylinders, can be explained by the difference in samples geometry. Indeed, in the case of cylinders, first, a larger volume is submitted to tensile stresses and, second, the cooling effect is probably more efficient.

Whatever the sample geometry is, one observes a significant ΔT_c decrease (approximately 70 K) when the nozzle section changes from 4.9 to 2.45 mm^2. This increase of the thermal shock severity results from a more efficient cooling of samples due to the increased air speed when the nozzle section decreases.

When the cooling is generated by two superposed nozzles of same section (2.45 mm^2), the cracking always arises for ΔT_c values lying between those obtained with single nozzles of 2.45 and 4.9 mm.

It is rather difficult to justify such a result on the basis of strict mechanical and thermal approaches. Nevertheless, from a qualitative viewpoint, one can think that it results from two combined actions:

- The speed of compressed air ranges between those obtained in the two limiting cases.
- The air turbulent flow at the sample periphery is more intense and induces more efficient thermal exchanges by forced convection.

5.1.1. Remarks

- The numerical values obtained for ΔT_c are close to those found by other authors for a similar material tested in similar experimental conditions.[5] They are much larger than those measured by quenching in cold[6,7] or hot[8] water, similar in magnitude to those obtained by quenching in a bath of silicon oil[9] and slightly lower to those obtained by quenching in a fluidised bed.[10] These comparisons allow us to consider the quench by compressed air as a mild thermal shock.
- The critical drop in temperature ΔT_c is limited by an asymptotic value when d increases. This proves the existence of a cooling "distant field" inside of which the convective effects due to the compressed air throws (forced convection) are not dependent on d. For much larger d values, the cooling would occur in free convection and, because of the lowering of the thermal shock severity, the critical temperature difference would increase.

5.2. Heat exchange coefficient h

5.2.1. Thermoelastic approach

The previous results can be examined in the frame of the thermo-elastic theory to approximate the magnitude of the superficial heat exchange coefficient. In the case of thermal exchanges by air, it may be thought that such a calculation will give a reasonable value of h, what is unrealistic for water quenching, because of the state changes of water arising in this case[11,12] at 100 °C.

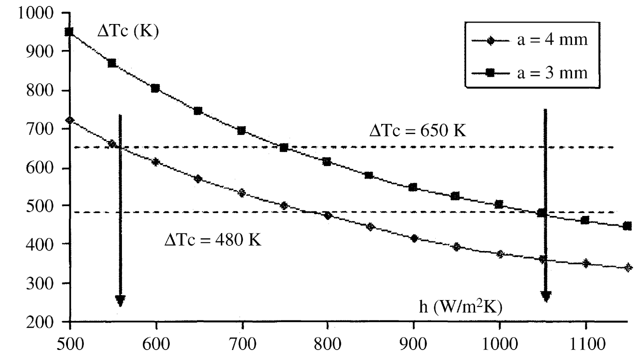

Fig. 4. Heat exchange coefficient estimated from the measured ΔT_c values.

For this rough calculation, the thermo-mechanical properties of material are considered less dependent on temperature and, because fracture occurs in mode 1, the first thermal shock parameter is calculated using the tensile strength. So, one obtains:

$$R = 42\,\mathrm{K} \tag{6}$$

The typical dimension, a, is an ambiguous parameter. Nevertheless, for a square section, its maximum value is the side of the square, that is to say $a = 4$ mm. Moreover the thermal conductivity is estimated from the range defined by ΔT_c where fracture occurs. Thus it becomes possible to calculate the stress reduction coefficient, Ψ, then the critical temperature difference, ΔT_c, versus h. By using the previous values, one obtains:

$$\Delta T_c = \frac{60.5 + 166.75\lambda}{(ah) - 19\,\exp(-16\lambda/(ah))} \tag{7}$$

The intercepts of the graph $\Delta T_c = f(h)$ with horizontals corresponding to the extreme values measured for ΔT_c give an estimation of the h range during the test.

The Fig. 4 represents the result thus obtained for samples of square section. Two graphs are plotted, which correspond respectively to typical dimensions a of 3 and 4 mm. One can conclude that, for the present experimental conditions, the heat exchange coefficient- lies between 550 (typical size 4 mm, three nozzles of 4.9 mm^2, $d > 15$ mm) and 1100 W/m^2 K (typical size 3 mm, three nozzles of 2.45 mm^2, $d = 2$ mm). This result is in good agreement with values found by others authors.[13]

5.2.2. Numerical approach

Thermal shocks have been simulated by taking into account the dependence of both elastic modulus E and thermal conductivity on temperature. In a first time, the spatio-temporal distribution of temperatures has been determined, then the mechanical response of the model to these loadings has been calculated. Iterative calculations have been performed by increasing the h values, until the maximal tensile stress (in the middle of each face) reaches the material strength in tension.

For square section bars (4 mm × 4 mm), two thermal loadings have been simulated whereas a single uniform thermal loading (normal to the external surface) has been simulated in the case of cylindrical samples ($\phi = 6$ mm).

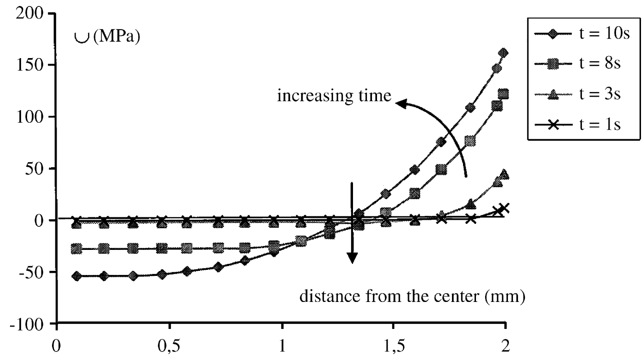

Fig. 5. Temperature profiles in a cross section of a squared sample ($d = 2$ mm).

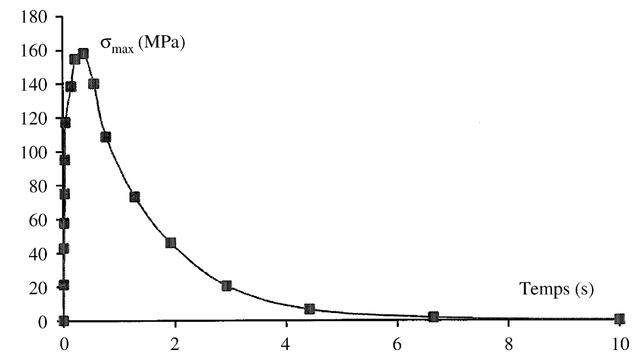

Fig. 6. Maximum value of the superficial tensile stress vs. time for a squared sample ($d = 2$ mm).

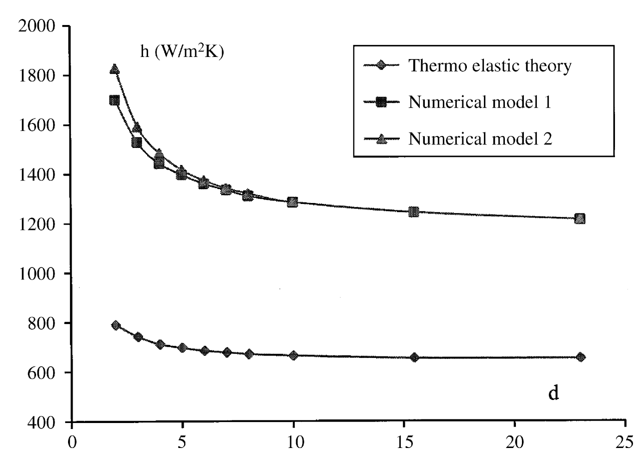

Fig. 7. Heat exchange coefficient estimated from the numerical simulation results (d cooling nozzle to sample distance).

For a square section sample, Figs. 5 and 6 illustrate results obtained for temperatures and stresses distributions. They agree very well with data of the literature[14] and show that the maximal stress is reached when the maximal temperature difference between specimen centre and surface is occurred. When the nozzles-sample distance is equal to 2 mm, it develops approximately 300 ms after the beginning of the cooling. Similar results are obtained in the case of cylindrical samples.

The Fig. 7 shows, as an example, typical variations of the superficial heat exchange coefficient h obtained by the numerical simulation and by application of the thermo-elastic theory. These results deal with a square section sample submitted to the cooling of three nozzles of 4.9 mm^2 section, but similar results have been obtained in all the other experimental cases.

One observes that the curves $h = f(d)$ thus obtained have the same general appearance, but that they give numerical values of h (for a given value of d) strongly dependent on the estimation method considered: the numerical simulation, *a priori*, the most reliable of the two methods, leads to h values approximately twice greater than those obtained by using the thermoelastic theory. Also application of thermoelastic model implies that, at surface sample, the temperature goes from T_i to T_f instantaneously: this assumption is physically impossible due to the fact heat transfer follows continuous laws and that thermal properties are finite values. Obviously, this disagreement is important in relative value, nevertheless it remains modest in absolute value and it is then possible to assert that values of h are limited to the range 550–2000 W/m^2 K for the experimental conditions of this study.

5.3. Cracking

The Fig. 8 illustrates the cracking development versus the imposed temperature difference. One distinguishes three stages that agrees perfectly with the energetic crack analysis proposed by Bahr and Weiss.[15]

- For $\Delta T = \Delta T_c$ (just critical shock), cracking develops on the main face only. The maximal tensile stress (in the middle of the face) is just sufficient to activate the greatest flaw present in the cooled zone. One finds the same situation in all the neighbour cross sections and, so, the activated' flaws in the middle of the face coalesce one observes a unique longitudinal crack whose propagation was typically unstable. A similar result is obtained in the case of water quench.[8]
- For $\Delta T > \Delta T_c$ (super critical thermal shock): many transversal cracks appear on all faces. The tensile stresses reach their maximal value more quickly and the energy to release increases: smaller flaws are activated which propagate first in an unstable manner then in a stable one.
- For $\Delta T \gg \Delta T_c$ (hyper-critical thermal shock): the cracking becomes total. The energy to release becomes very large and even very small flaws are activated. These small flaws being numerous, one observes longitudinal and transversal cracks on all the faces. The crack density increases with the imposed difference temperature and one observes a crack density of the main face greater than on the other faces.

The experimental tests have been confirmed different results.[16] One can therefore assert that the main face undergoes the most severe thermal shock:

- for $\Delta T = \Delta T_c$, it is the single face where cracking occurs;
- for $\Delta T > \Delta T_c$, its crack density is the most important;
- for $\Delta T \gg \Delta T_c$, its crack becomes catastrophic.

The depth of longitudinal cracks which develop during a critical thermal shock can be estimated by means of numerical

Fig. 8. Typical crack patterns after critical and super critical thermal shocks.

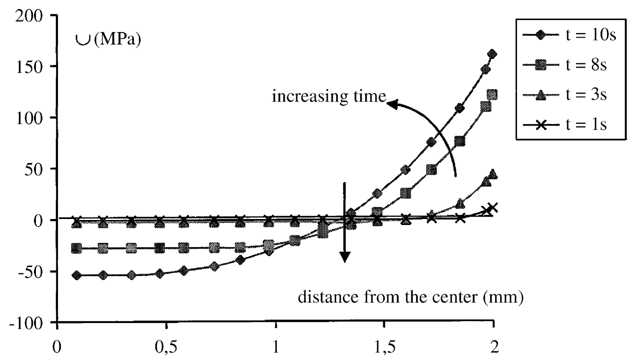

Fig. 9. Stress profiles vs. time in a cross section of a squared sample.

simulation. First, temperature distribution bas been determined with an iterative calculation, then stress distribution has been calculated at these loadings: stresses versus half thickness are plotted each increase time. Fig. 9 represents, at various times, the stress variations in the half thickness of a bar. One observes that the transition between the tensile zone and the compressive one is located at approximately 0.7 mm to the outer surface. By assuming that cracks cannot propagate into the compressive zone, it is possible to say that the crack depth inside the sample is, at the most, 0.7 mm. Nevertheless, by sawing samples having endured a just critical thermal shock, then by observing them with a binocular magnifying glass, one observes an average penetration greater to this value. The crack growth during cutting is avoided because cracks cannot propagate into the compressive zone.

In a first time, one can therefore admit that the average crack depth is about one millimeter. The Fig. 8 shows that the length of this crack is approximately 25 mm, what allows to estimate to 50 mm^2 the area of the new surfaces created during the thermal shock.

The surface energy of the material being approximately 20 J/m^2,[13] it appears that the energy released by creation of surfaces during a critical shock is extremely low ($20 \times 50 \times 10^{-6}$ J, that is to say approximately 1 mJ) and, in any case, very lower to the elastic strain energy which is, here, of about a 10 mJ.

6. Conclusion

The experimental study of the thermal shocks resistance of a polycrystalline alumina has been performed by quenching samples of square and circular section in a flow of compressed air.[17] According to the intensity of convective heat exchanges and to the samples geometry, the critical temperature difference, ΔT_c, varies from 480 (cylindrical samples submitted to a vigorous cooling) to 650 K (prismatic samples to squared section submitted to a moderate cooling), what allows us to consider the imposed solicitations as mild thermal shocks.

The same critical thermal shocks have been simulated by means of a finite elements code in which the value of the superficial heat exchange coefficient, h, was increased until the maximal calculated tensile stress reaches the strength of the material. For the experimental conditions developed, one access thus, in indirect manner, to h values ranging between 1250 and 1850 W/m^2 K. These values are in good agreement with those obtained by other authors by using different approaches.

The crack density increases with the imposed temperature difference and the cracking evolution agrees the model proposed by Bahr and Weiss.

Acknowledgements

The authors would like to thank the Ecole Nationale Superieure d'Ingenieurs de Limoges for its support in the use of the FEM code ABAQUS.

References

1. Kingery, W. D., Factors affecting thermal stress resistance of ceramic materials. *J. Am. Ceram. Soc*, 1955, **38**(1), 3–15.
2. Hasselman, D. P. H., Unified theory of thermal shock fracture initiation and crack propagation in brittle materials. *J. Am. Ceram. Soc*, 1969, **52**(11), 3600–3604.
3. Glandus, J. C., *Rupture fragile et résistance aux chocs thermiques dé ceramiques á usages mecaniques*. Thesis. Université de Limoges, 1981.
4. Tranchand, V., *Simulation Informatique de Chocs Thermiques Durs et de la Fatigue Thermique*. Thesis. Université de Limoges, 1993.
5. Saadaoui, M., *Contribution á l'etude du comportement thermomecanique des materiaux ceramiques a effet de courbe R. Cas du choc et de la fatigue thermiques*. Thesis. Ecole d'Ingénieurs Mohammadia, Rabat, 1996.
6. Davidge, R., Thermal shock and fracture in ceramics. *Trans. Br. Ceram. Soc*, 1967, **66**(8), 405–422.
7. Gupta, T. K. P., Strength degradation and crack propagation in thermally shocked alumina. *J. Am. Ceram. Soc.*, 1972, **55**(5), 249–253.
8. Glandus, J. C. and Tranchand, V., Thermal shock by water quench: numerical simulation. Thermal shocks and thermal fatigue of advanced ceramics. In *NATO Science Series E: Appl. Sci.* (*Vol 241*), eds. G. A. Schneider and G. Petzow. 1993, pp. 307–316.
9. Hasselman, D. P. H., Effect of surface-compression strengthening on thermal stress fracture of brittle ceramics. *Proc. Sci. Ceram.*, 1973, **7**, 107–122.
10. Niihara, K., Singh, J. P. and Hasselman, D. P. H., Observations on the characteristics of a fluidized bed for the thermal shock testing of brittle ceramics. *J. Mater. Sci.*, 1982, **17**, 2553–2559.
11. A. Gaudon, Etude expérimentale et numérique de la résistance aux chocs thermiques de ceramiques thennomécaniques. Thesis. Université Paul Sabatier, Toulouse, 1993.
12. Singh, J. P., Tree, Y. and Hasselman, D. P. H., Effect of bath and specimen temperature on the thermal stress resistance of brittle ceramics subjected to thermal quenching. *J. Mater. Sci.*, 1981, **16**, 2109–2118.
13. P. Peigne, Résistance aux chocs thermiques de céramiques thermomécaniques. Thesis. INSA, deLyon, 1991.

14. N. Tessier-Doyen, Etude expérimentale et numérique du comportement thermomécanique de matériaux réfractaires modéles. Thesis. Université de Limoges, 2003.
15. Bahr, H. A., Fisher, G. and Weiss, H. J., Thermal shock crack patterns explained by single and multiple crack propagation. *J. Mater. Sci.*, 1986, **21**, 2716–2720.
16. Collin, M. and Rowcliffe, D., The morphology of thermal cracks in brittle materials. *J. Eur. Ceram. Soc.*, 2002, **22**(4), 435–445.
17. Bao, Y. W., Wang, X. H., Zhang, H. B. and Zhou, Y. C., Thermal shock behaviour of Ti_3AlC_2. *J. Eur. Ceram. Soc.*, 2005, **25**(14), 3367–3374.